JOC The Journal of Organic Chemistry

Article

pubs.acs.org/joc

Impact of Alkyl Substituents on the Gas-Phase Competition between Substitution and Elimination

Keyanna M. Conner and Scott Gronert*

Department of Chemistry, Virginia Commonwealth University, Richmond, Virginia 23284, United States

Supporting Information

ABSTRACT: The S_N2 and E2 reactions of a series of alkyl bromides with varying substitution patterns at the α- and β-carbons have been studied in the gas phase using naphthoate and phenoxide-based nucleophiles. The experimental work is supported by calculations at the MP2/6-31+G(d,p)//MP2/6-31+G(d) level. The results parallel reactivity patterns observed in the condensed phase, but offer new insights into steric factors in S_N2 processes. In the gas phase, polarizability is more important, and the highest S_N2 reactivity is observed when the β-carbon is 2°. In addition, the data confirm that alkyl substituents at the β-carbon have a greater accelerating effect on E2 reactions than those at the α-carbon. Finally, computed data based on lowest enthalpy pathways provide poor descriptions of the reactions of the larger alkyl bromides and are skewed toward crowded systems that offer stabilizing, nonbonded interactions at the expense of conformational freedom.

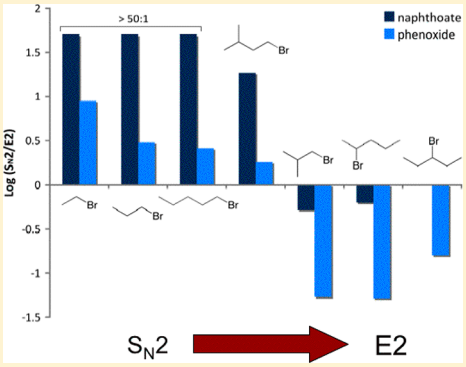

INTRODUCTION

The competition between substitution (S_N2) and elimination (E2) in nucleophilic reactions of alkyl halides has had a profound influence on the development of physical organic chemistry[1,2] and remains an important testing ground for identifying reactivity patterns in gas-phase organic chemistry.[3] Several groups have probed these reactions to investigate various factors that influence the reactivity, including substrate structure, nucleophilicity, solvent effects, the α-effect, and kinetic isotope effects.[4−17]

We have previously investigated a simple set of alkyl bromides with varying substitution patterns.[7,18] The set included ethyl and *n*-propyl (primary), isopropyl and *sec*-butyl (secondary), and *tert*-butyl (tertiary) substrates. Product distributions were reported for these substrates with dianions bearing either a phenoxide or benzoate as the nucleophilic site, and the results were consistent with reactivity trends typically observed in the condensed phase. With the benzoate, primary substrates gave mainly substitution, secondary substrates produced a roughly even mixture of substitution and elimination, and tertiary substrates gave mainly elimination. In the case of the stronger base, the phenoxide nucleophile, there is an overall greater prevalence of elimination throughout the series. Kinetic data for these reactions showed rate increases from 1° to 2° to 3° substrates, with E2 processes reaching higher overall efficiencies in the highly substituted systems. Methylation at the β-carbon enhanced S_N2 partial rates indicating that the advantages of greater polarizability could overcome steric effects in the gas phase.[15,17,19,20]

We now return to these types of systems and present a more comprehensive set of alkyl bromides with a wider variation of substitution patterns at both the α- and β-carbons (Scheme 1). The goal of this study is to explore the effect of α- versus β-alkyl substitution on the preferred mechanistic pathways and reaction kinetics. This current series includes a neopentyl system, 1-bromo-2,2-dimethylpropane. Although the S_N2 reactions of neopentyl systems are very slow in the condensed phase, there are examples of fast S_N2 reactions on neopentyl halides in the gas phase when small, basic nucleophiles such as fluoride and methoxide are used.[6] As in our previous studies, a quadrupole ion trap mass spectrometer was used to obtain experimental data, which is supported by computational work. In contrast to the previous work, we are employing a second generation of dianion nucleophiles and as a result, we report new data with these nucleophiles for the previous alkyl halides.

RESULTS

Reaction Systems. As in previous studies, dianion nucleophiles are used in this study. The dianion design utilizes a common architecture, containing aryl spacer groups and a chemically inert anionic site, Z^-, along with a nucleophilic anionic site, Y^-.[7] The advantage of the second charge is that the nucleophile retains a charge after the reaction and can be identified by mass spectrometry. This is contrary to singly charged nucleophiles where both pathways, E2 and S_N2, lead to the same ionic product, which is generally a halide ion (Scheme 2). The dianions used in this study are shown in Scheme 3.

We have shown in the past that when the distance between the two charges in the dianion is roughly 15 Å or more, the barrier for a process like an S_N2 reaction is only slightly lower than that of the singly charged analogue because only a small

Received: June 19, 2013
Published: July 29, 2013

dx.doi.org/10.1021/jo4013354 | J. Org. Chem. 2013, 78, 8606−8613

Scheme 1. Set of alkyl bromides substituted at α and β-carbons

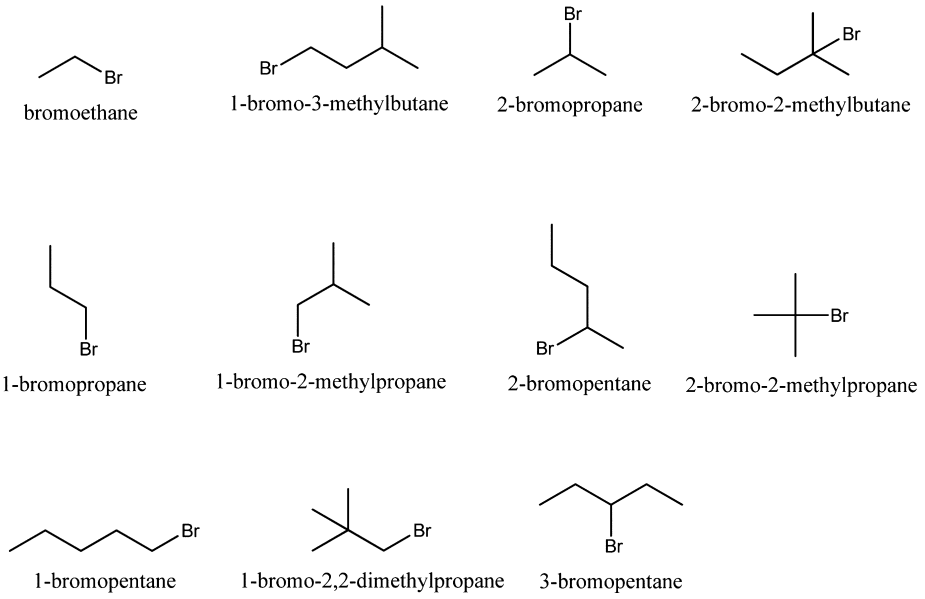

Scheme 2. Dianion Products

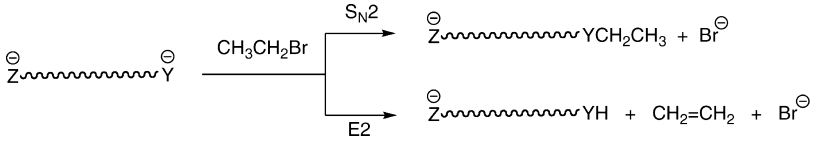

Scheme 3. Dianions Employed in This Study

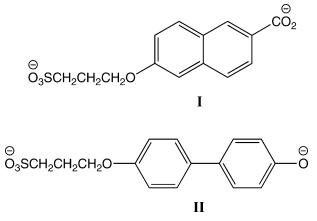

fraction of the internal electrostatic repulsion is released at the transition state; the transition state is very early on the reaction coordinate for charge separation.[21] Therefore, dianions can be suitable surrogates for studying the chemistry of singly charged analogs. In this study, the naphthoate dianion, **I**, is the less basic of the two nucleophiles and has a computed proton affinity (PA) of 367 kcal/mol for protonating the carboxylate anion (MP2/6-31+G(d,p)//MP2/6-31+G(d)). The phenoxide dianion, **II**, has a computed PA of 371 kcal/mol. Both of these are considerably larger than the computed PAs for singly charged analogues, 2-naphthoate (336 kcal/mol) and phenoxide (348 kcal/mol, exp = 350 kcal/mol[22]). The differences come from the fact that the dianions release about 25−30 kcal/mol of internal electrostatic repulsion when one of their charges is neutralized. As noted above, the transition states in these systems occur extremely early relative to the charge separation process, so the PA of the singly charged analogue is a better measure of the effective kinetic reactivity of the dianion

Table 1. Rate Constants for Dianion I and Computed Barriers for Benzoate[a]

	α-carbon	β-carbon	k	$k(S_N2)^b$	$k(E2)^b$	barrier S_N2	barrier E2	$k(E2)/H_\beta{}^c$
bromoethane	1°	1°	0.090	0.090	<0.001	−1.0	8.0	
1-bromopropane	1°	2°	0.138	0.137	0.001	−2.1	4.6	0.0005
1-bromopentane	1°	2°	0.50	0.49	0.01	−2.1	4.1	0.005
1-bromo-3-methylbutane	1°	2°	0.58	0.5	0.03	−3.4	2.2	0.015
1-bromo-2-methylpropane	1°	3°	0.070	0.024	0.046	−0.7	1.3	0.046
1-bromo-2,2-dimethylpropane	1°	4°	NR			4.8		
2-bromopropane	2°	1°	NR			2.1	6.9	
2-bromopentane	2°	1°, 2°	0.26	0.10	0.16	0.5	2.6	0.16
3-bromopentane	2°	2°	0.20	0.10	0.10	−1.0	3.4	0.05
2-bromo-2-methylpropane	3°	1°	0.07	<0.001	0.07	10.4	5.9	0.008
2-bromo-2-methylbutane	3°	1°, 2°	1.32	<0.01	1.32	8.4	3.1	0.66

[a]Units are 10^{-10} cm^3 molecule^{-1} s^{-1}. NR = no reaction. Relative energies in kcal/mol at the MP2/6-31+G(d,p)/MP2/6-31+G(d) level. Includes Hartree−Fock ZPE correction scaled by 0.9135. [b]Partial rate for each channel. [c]The E2 rate is scaled by the number of β-hydrogens on the most highly substituted β-carbon (e.g., 2 for 2-bromopentane).

dx.doi.org/10.1021/jo4013354 | J. Org. Chem. 2013, 78, 8606−8613

Table 2. Rate Constants for Dianion II and Computed Barriers for Phenoxide[a]

	α-carbon	β-carbon	k	$k(S_N2)^b$	$k(E2)^b$	barrier S_N2	barrier E2	$k(E2)/H_\beta{}^c$
bromoethane	1°	1°	0.096	0.089	0.007	−3.3	2.0	0.002
1-bromopropane	1°	2°	0.194	0.146	0.048	−3.6	−1.4	0.024
1-bromopentane	1°	2°	0.89	0.64	0.25	−3.7	−2.7	0.12
1-bromo-3-methylbutane	1°	2°	1.03	0.66	0.37	−4.6	−4.5	0.18
1-bromo-2-methylpropane	1°	3°	0.59	0.03	0.56	−2.8	−3.6	0.56
1-bromo-2,2-dimethylpropane	1°	4°	NR			3.6		
2-bromopropane	2°	1°	0.091	0.017	0.074	−0.8	1.2	0.01
2-bromopentane	2°	1°, 2°	2.64	0.13	2.51	−4.0	−4.4	2.51
3-bromopentane	2°	2°	1.78	0.25	1.53	−5.2	−2.1	0.76
2-bromo-2-methylpropane	3°	1°	0.29	<0.003	0.29	5.9	0.4	0.03
2-bromo-2-methylbutane	3°	1°, 2°	4.80	<0.05	4.80	3.4	−2.7	2.40

[a]Units are 10^{-10} cm^3 molecule^{-1} s^{-1}. NR = no reaction. Relative energies in kcal/mol at the MP2/6-311+G(d,p)/MP2/6-31+G(d) level. Includes Hartree−Fock ZPE correction scaled by 0.9135. [b]Partial rate for each channel. [c]The E2 rate is scaled by the number of β-hydrogens on the most highly substituted β-carbon (e.g., 2 for 2-bromopentane).

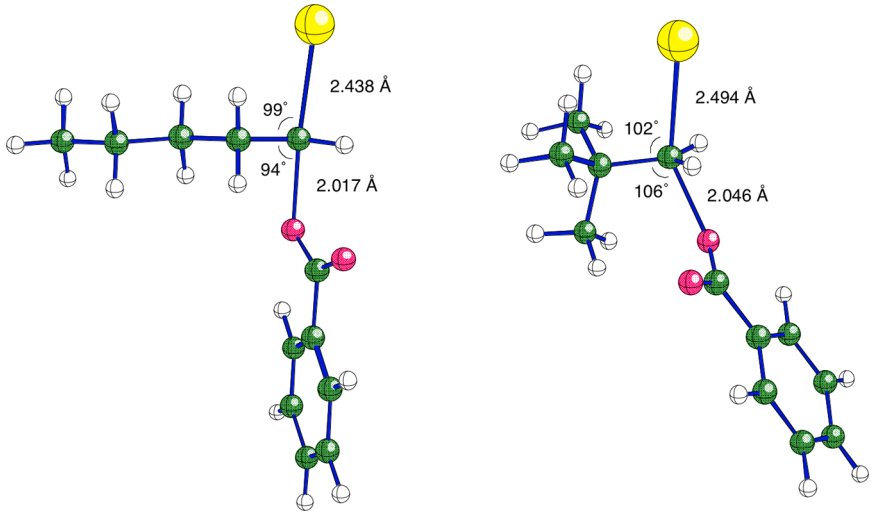

Figure 1. MP2/6-31+G(d)-optimized geometry for S_N2 reactions of benzoate with 1-bromopentane (left) and 1-bromo-2,2-dimethylpropane (right). Key: carbon, green; oxygen, red; bromine, yellow; hydrogen, white.

nucleophile (most of internal electrostatic repulsion is released after the transition state).

Rate constants and computed barriers (MP2/6-31+G(d,p)//MP2/6-31+G(d)) are shown in Tables 1 and 2. In the E2 reactions, the listed barriers are for formation of the most stable alkene (E stereochemistry and most highly substituted, where applicable). For perspective, collision rates of about (3−4) × 10^{-9} cm^3 molecule^{-1} s^{-1} are expected for these systems.[23,24] The reported data suggest that these systems tend to give one successful reaction in every 10 to several hundred collisions. To limit the computational demands of the theoretical studies, the dianions are modeled by simpler, singly charged nucleophiles. Benzoate is used for the naphthoate dianion, **I**, and phenoxide for the phenoxide dianion, **II**. This approach has been used previously with good success.[25−27]

The reactions are expected to proceed through double-well potentials where the first well corresponds to the formation of an ion−dipole complex.[4] The system rises from this complex over the S_N2 or E2 barrier leading to a product complex in the second well. Because the initial complexation energy can be greater than the mechanistic barrier, the transition states often are below the energy of the separated reactants and negative overall activation barriers are observed.

DISCUSSION

S_N2 Reactions. The S_N2 rate constants for both nucleophiles follow the expected pattern in the progression from 1° to 3° at the α-carbon. There is roughly a 5-fold drop in the S_N2 rate constant going from 1° to 2° centers, and then at least a 50-fold drop in going to a 3° center (no S_N2 reactions are observed within our dynamic range for 3° bromides). As expected, the more basic nucleophile, **II**, gives higher rate constants (by a factor of about 2). The next question is the impact of substituents at the β-carbon. In the condensed phase, bulk at the β-carbon generally reduces S_N2 rates. For example, the relative rates for bromide exchange in acetone for bromoethane, 1-bromopropane, and 1-bromo-2-methylpropane are 1, 0.65, and 0.033, respectively.[1] In the gas phase, it can be seen that a 2° center at the β-carbon can enhance the S_N2 rate (bromoethane vs 1-bromopropane and 1-bromopentane), even in the presence of additional branching (e.g., 1-bromo-3-methylbutane). As noted above, this has been observed in the past and is likely the result of the β-substituent increasing the polarizability of the substrate in the vicinity of the reaction center while imposing limited steric interactions with the bare, unsolvated nucleophilic center. The situation is different when the β-carbon becomes tertiary or quaternary (1-bromo-2-methylpropane and 1-bromo-2,2-dimethylpropane). In the

dx.doi.org/10.1021/jo4013354 | J. Org. Chem. 2013, 78, 8606−8613

former (isobutyl), there is an S_N2 rate decrease for both nucleophiles, and for the latter (neopentyl), we see no reaction on our time scale with either nucleophile. Previously, gas-phase S_N2 reactions have been seen with neopentyl halides, but the nucleophiles were small and highly basic (fluoride and methoxide).[6] Apparently, the more crowded nucleophiles in the present study exceed the steric capacity of the neopentyl reaction path.

In the computed data, there is a general increase in the S_N2 barrier in the progression from 1° to 3° centers at the α-carbon for the benzoate model nucleophile. The key and expected exception is the neopentyl system,1-bromo-2,2-dimethylpropane, which has a much higher barrier than the other 1° halides. The computed barriers for both 1-bromo-2,2-dimethylpropane and 2-bromo-2-methylbutane (the 3° halides) are sufficiently large to prevent an observable reaction with either nucleophile in our experimental system. The problems for the neopentyl system can be seen in the MP2/6-31+G(d) optimized geometry of the transition state of its S_N2 reaction with benzoate (Figure 1). It indicates that a crowded β-carbon distorts the pathways for the nucleophile and leaving group − the angles at the carbon differ significantly from the 90° expected for a trigonal bipyramid. The corresponding transition state for 1-bromopentane is included for comparison. The unexpected outcome in the computed data is that the S_N2 barriers for 2-bromopentane and 3-bromopentane are surprisingly close to those for the 1° alkyl halides. This effect is more pronounced when phenoxide is the model nucleophile and the computed S_N2 barrier for 3-bromopentane is well below the barriers for the unhindered 1° alkyl halides. In this respect, the computed data directly conflict with the gas-phase experimental data as well as generalities derived from condensed-phase substitutions; clearly, the computed barriers are not giving a realistic picture of the S_N2 process in these systems. This has not been observed in our previous comparisons of computed and experimental data.[25−27]

The overriding issue is that the computed barriers are for the saddle point on the electronic energy surface. Structures that maximize stabilizing, nonbonded interactions are favored on this surface, and there is no penalty for a highly ordered structure with limited flexibility. In other words, entropic considerations are completely ignored from both a conformational and phase space perspective. Although this does not appear to be a significant issue when dealing with small systems with a limited number of conformations and weak, long-range nonbonded interactions, this is not the case in the pentanes. The lowest energy transition state for the reaction of phenoxide with 3-bromopentane is shown in Figure 2 and it can be seen that there are a number of midrange, nonbonded interactions between the phenyl ring and pentyl group. Interactions between an ortho hydrogen of the phenoxide and hydrogens on carbons 1 and 3 of the 3-bromopentane are highlighted. Although stabilizing, these interactions would be very sensitive to the geometry and unavailable in other conformations. To probe this issue, a more extensive survey of the potential energy surfaces was completed for the S_N2 reactions of phenoxide with 1-bromopentane and 3-bromopentane. Specifically, the conformational search routine in Spartan 10[28] was used to identify all likely transition states for these reactions. The conformers were identified using the MMFF force-field and the software's systematic algorithm. For the transition states, the bond lengths and angles at the reaction center were constrained to match expectations for an S_N2 reaction. Identical conformers were excluded by the search algorithm. The same approach was used to identify the likely conformations of the bromoalkanes. Each of the conformations was then optimized at the MP2/6-31+G(d) level and a frequency calculation was completed. The combined partition function data from these calculations provides a rough estimate of the likelihood of reaching the product across all the reasonable pathways. Overall, such an analysis suggests that the 1-bromopentane system offers more low energy S_N2 paths to products. For the 3-bromopetane system, this analysis indicates that nearly 30% of the reaction probability is concentrated in a single path with only 10 pathways having at least a 3% fraction of the reactivity. In contrast, the 1-bromopentane system has 16 pathways that contribute at least 3%, with no pathway contributing more than 13% to the overall reactivity. The analysis also suggests that the S_N2 reaction of phenoxide with 1-bromopentane is 3 times more likely than that with 3-bromopentane despite the presence of a lower energy pathway (enthalpically) on the latter's surface.[29] Although a full dynamics analysis would be preferred, it is not practical for a bimolecular system of this size. The present results, though approximate in nature, provide a rationalization for the discrepancy between the computed lowest energy paths and the observed kinetics. They also highlight that the strong influence of favorable, nonbonded interactions in large gas-phase systems can lead to unrepresentative results if the analysis is limited to lowest energy pathways, particularly if entropy effects are not included in identifying the lowest energy path. In addition, it is known that gas-phase S_N2 reactions can have nonstatistical behavior, which could also contribute to the discrepancies between experiment and theory in these systems.[30−32]

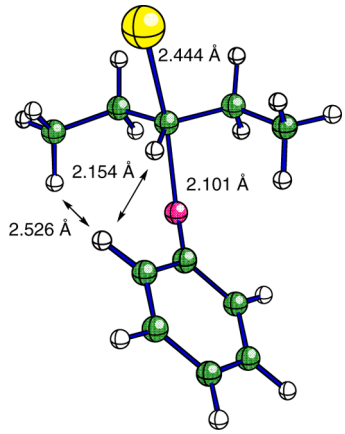

Figure 2. MP2/6-31+G(d)-optimized geometry for S_N2 of reaction of phenoxide with 3-bromopentane. Key: carbon, green; oxygen, red; bromine, yellow; hydrogen, white.

E2 Reactions. The E2 rate constants are very sensitive to the nucleophile, and the more basic dianion, **II**, has rate constants that are generally about an order of magnitude higher. The sensitivity of E2 reactions to base strength is well established[2] and clearly related to the importance of the proton transfer component of the reaction. This effect is seen in the computational data, which indicates a 6 ± 1 kcal/mol drop in the E2 barrier in going from benzoate to phenoxide as the base.

The rate constants for the E2 processes span a large range for each nucleophile. For **I**, most of the 1° bromides give no E2 yield (rates $<10^{-13}$ cm^3 molecule^{-1} s^{-1}), and only 2-bromo-2-methylbutane has a rate constant that exceeds an estimated efficiency of 1% (efficiency = rate/estimated collision rate).

dx.doi.org/10.1021/jo4013354 | J. Org. Chem. 2013, 78, 8606−8613

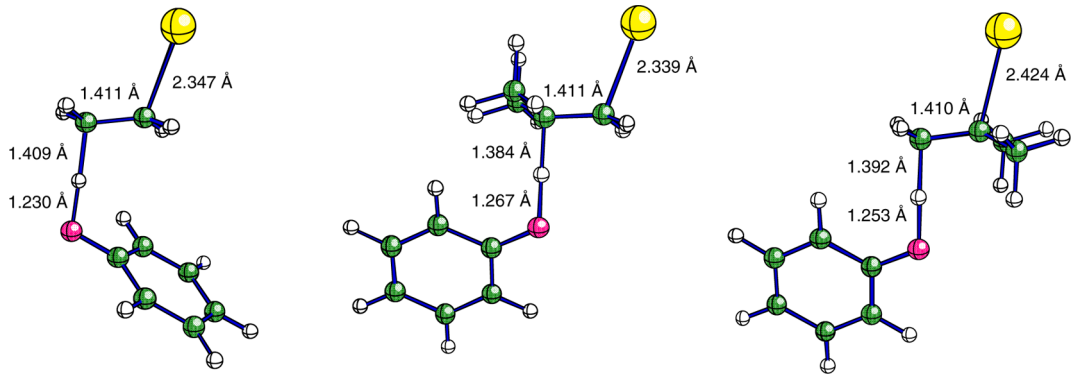

Figure 3. MP2/6-31+G(d)-optimized geometries for E2 transition states of the reactions of phenoxide with bromoethane (left), 1-bromo-2-methylpropane (middle), and 2-bromo-2-methylpropane (right). Key: carbon, green; oxygen, red; bromine, yellow; hydrogen, white.

With dianion **II**, rate constants were obtained for all the alkyl bromides with a β-hydrogen and span from 7×10^{-13} to 4.8×10^{-10} cm^3 molecule^{-1} s^{-1}. This range is much broader than what was observed in the S_N2 reactions of the 1° and 2° alkyl bromides (no S_N2 reactions were observed with 3° bromides).

Compared to the S_N2 reactions, the E2 reactions seem to have a more complicated relationship between the substitution patterns at the α- and β-carbons and the rate constants, but this is partly due to the varying number of β-hydrogens (i.e., the number of degenerate paths). When the rate constants are scaled by the number of β-hydrogens, clear patterns emerge. In this scaling, only the most reactive β-hydrogens are considered (i.e., those leading to the most highly substituted *E*-alkene product). The data below support this decision. Starting with bromoethane, addition of a methyl group at the α-position, 2-bromopropane, increases the E2 rate constant with **II** by a factor of roughly 5. Addition of a methyl group at the β-carbon, 1-bromopropane, increases the E2 rate constant with **II** by a factor of about 10. Here, both centers are going from 1° to 2° in the modification. Similar effects are seen in going from 2° to 3° centers. With **II**, the E2 rate constants increase about 3-fold in going from 2-bromopropane to 2-bromo-2-methylpropane and about 20-fold in going from 1-bromopropane to 1-bromo-2-methylpropane. The effect is also seen in the computed data, and the addition of a β-methyl group lowers the E2 barrier by 1−2 kcal/mol more than the addition of an α-methyl group. Despite being viewed as an electron-donating group, the β-methyl is capable of stabilizing the developing π-bond in the presence of carbanion character at the β-carbon. In addition, the polarizability of the β-methyl group is able to stabilize the charge on the incoming nucleophile. The small effect of methyl groups at the α-carbon indicates that these systems cannot take advantage of E1-character in the transition state (see below).

The geometries of the E2 transition states are relatively insensitive to the presence of alkyl substituents. In Figure 3, the parent system, bromoethane, as well as two extreme examples, 1-bromo-2-methylpropane and 2-bromo-2-methylpropane, are presented. In one extreme case, the α-carbon is 1° and the β-carbon is 3°, whereas in the other, the situation is reversed. Despite the reversal of the substituent pattern and different computed barriers (2.0, −3.6, and 0.4 kcal/mol, respectively), the transition states are similar, and not very different from the parent system − bromoethane has a slightly more advanced proton transfer component and the 2-bromo-2-methylpropane system seems to have a somewhat later transition state, but this is very subtle. There is no indication that the alkyl substituents are moving the transition states significantly along the E1-like → E2 → E1$_{cb}$-like spectrum; they all appear to be relatively synchronous E2 transition states. In contrast, our previous work with electron-withdrawing substituents at the β-carbon indicated large changes in transition state geometries and very significant shifts toward E1$_{cb}$-like transition states.[25] Finally, the structures in Figure 3 exhibit varying orientations for the phenyl group − the potential for rotation around the forming O−H bond is very flat, and it appears that subtle differences in midrange vdW interactions drive the preferences.

As in the S_N2 data, the computational modeling reproduces the experimental trends with the smaller alkyl bromides, but there are some discrepancies with the larger ones. For example, the lowest E2 barriers with phenoxide are for 2-bromopentane (formation of E-2-pentene) and 1-bromo-3-methylbutane, but the observed rate constants with **II** do not follow this pattern, particularly 1-bromo-3-methylbutane, which gives an E2 reaction that is 15 times slower than that of 2-bromo-2-methylbutane, despite having a barrier that is predicted to be 1.8 kcal/mol lower. The reason for the discrepancy is undoubtedly related to what was observed in the S_N2 systems. The systems with extensive branching at the β-carbon can adopt transition states that maximize favorable nonbonded interactions with the nucleophile, but this leads to an entropically unfavorable pathway with limited conformational freedom.

Calculations were also completed for transition states leading to the less substituted alkene in the case of 2-bromopentane and 2-bromo-2-methylbutane. The computed barriers for forming the less substituted alkenes are 3−5 kcal/mol higher, and one does not expect these pathways to be competitive. This outcome was expected and is consistent with the general impact of alkyl substituents on E2 barriers. As noted above, the computed E2 barriers for 1-bromopropane are about 3 kcal/mol lower than those for bromoethane. This effect is also illustrated in the dramatic difference in the observed E2 rate constants for 2-methyl-2-bromobutane and 2-methyl-2-bromopropane, where addition of the β-methyl group leads to a multifold rate increase.

Competition between S_N2 and E2 Reactions. In these systems, the rate constants are less than 10% of the expected collision rate, so the product distributions should principally be controlled by the reaction barriers. There is a delicate balance between the two mechanisms and in many of the substrates, one path represents 90% or more of the reactivity. The mechanistic preference is influenced by the substituents at the

dx.doi.org/10.1021/jo4013354 | J. Org. Chem. 2013, 78, 8606−8613

α- and β-carbon as well as the basicity of the nucleophile. When both of these factors favor one mechanism, it dominates, but when they counter each other, a product mix is seen. In Figure 4, simple heat maps based on the alkyl substitution patterns are

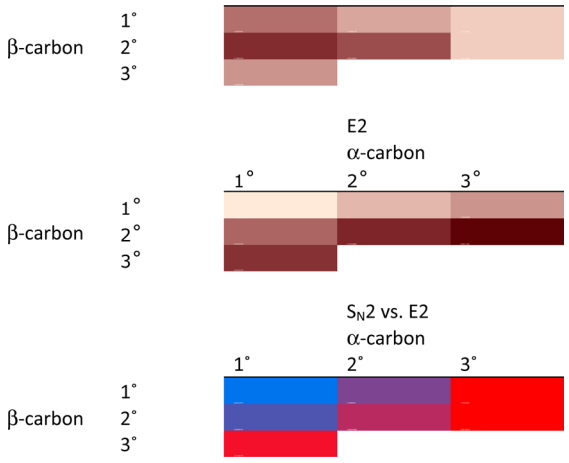

Figure 4. Heat maps for S_N2 and E2 reactivity. Data based on rate constants from the reactions with **II**. E2 rates are on a per β-hydrogen basis. For individual reactions, color intensity correlates with log(k). Lightest color corresponds to no observed products. For the comparison of mechanisms, the difference in log(k) is plotted with blue symbolizing S_N2 and red symbolizing E2. Dark blue indicates that S_N2 dominates, dark red indicates that E2 dominates, and purple indicates a mix of S_N2 and E2. White indicates no example was investigated in the study.

given for the S_N2 and E2 reactions of **II** with sample substrates. The patterns for the S_N2 and E2 reactions are, as expected, quite different. In the gas phase, the S_N2 reactivity is maximized in the substrates where the β-carbon is 2°, with the highest rates occurring when the α-carbon is 1°. This suggests that the steric impact of a 2° center at the β-carbon is tolerable in the gas phase and is outweighed by the advantages of the added, local polarizability that comes with greater substitution. The case where both centers are 1° (bromoethane) does not give the highest rate constant because it lacks the polarizability of the larger, but more crowded substrates containing a 2° β-carbon. The pattern is simple with E2 reactions and the reactivity increases in moving toward the lower right quadrant where substitution increases at both the α- and β-carbons. A heat map of the numerical difference in the logarithms of the S_N2 and E2 rate constants is also given in Figure 4 and the competition is most evenly balanced in the center of the plot where both the α- and β-carbons are 2°. Taken together, the plots in Figure 4 highlight that the shift from the S_N2 to the E2 mechanism is driven by both a decrease in S_N2 rate constants combined with an increase in E2 rate constants with greater alkyl substitution.

As has been noted before, E2 reactions are more sensitive to the basicity of the nucleophile than S_N2 reactions.[2,7] The current data set provides excellent examples of this effect. With 3-bromopentane, the S_N2 rate constant increases by a factor of 2.5 in switching to dianion **II**, whereas the E2 rate constant increases by a factor of 15. Similar differential effects are seen in 2-bromopentane, 1-bromo-3-methylbutane, and 1-bromo-2-methylpropane. This leads to a significant shift toward the E2 process with the stronger base (Figure 5). In each example, there is a multifold decrease in the S_N2 to E2 ratio when **II** is the base. The same trends are seen in the computed data and the shift to the stronger base reduces the S_N2 barrier by about half the amount seen for the E2 reactions (2–3 kcal/mol vs 6–8 kcal/mol).

SUMMARY

Overall, the present results provide further evidence that gas-phase and condensed-phase systems exhibit similar trends in S_N2 and E2 reactivity despite having very different potential energy surfaces and absolute rate constants. Here, the effect of varying the number of alkyl substituents at the α- and β-carbon was probed. For the S_N2 process, the data highlight that in the absence of solvation, the steric demand of the nucleophile is reduced and processes with a 2° center at the β-carbon are favored by the greater polarizability of the more highly

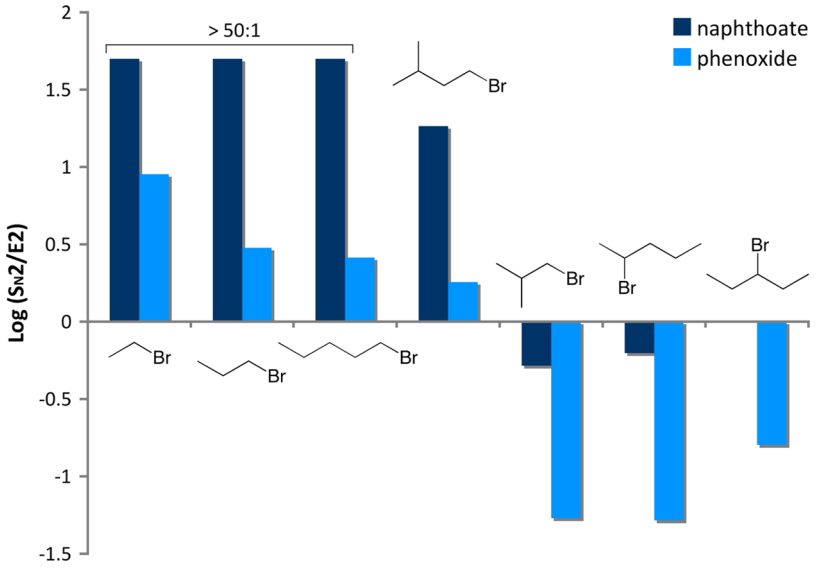

Figure 5. Log of the ratio of S_N2 to E2 rate constants of alkyl bromides with naphthoate (**I**) and phenoxide (**II**) dianion. In cases where no E2 product is seen, a ratio of 50:1 is plotted (bromoethane, 1-bromopropane, and 1-bromopentane with **I**). Systems that give no reaction with a nucleophile (2-bromopropane) or all E2 reactivity (2-bromo-2-methylpropane and 2-bromo-2-methylbutane) were excluded.

dx.doi.org/10.1021/jo4013354 | J. Org. Chem. 2013, 78, 8606–8613

substituted substrate; the polarizability effect is also leveraged in the gas phase by the low dielectric of the medium. However, a tertiary or a quaternary center at the β-carbon offers sufficient steric bulk to reduce or quench the S_N2 reactivity in our systems. The E2 reactions follow the typical pattern seen in the condensed phase, with reactivity increasing with additional substituents at the α- or β-carbon. In contrast to earlier work with small systems, the current data cannot be computationally modeled with a simple ab initio approach based on the lowest energy (electronic + zero-point energy) transition state. The larger systems are able to adopt highly ordered transition states that maximize nonbonded interactions but in fact are likely to represent only a limited part of the accessible phase-space for the reaction process. When a full suite of likely pathways is considered, including entropic effects, the computational modeling is consistent with measurements on the corresponding experimental systems. This result highlights the approximate nature of modeling reactions with lowest energy pathways and suggests that more comprehensive surveys of the potential energy surface are needed to model systems of modest size, such as the pentyl bromides in this report.

METHODS

Mass Spectrometry. All experiments were performed in a quadrupole ion trap mass spectrometer (modified ThermoFinnigan LCQ DECA) equipped with electrospray ionization (ESI).[2] All dianions were generated using electrospray ionization. The parent dianions were dissolved in methanol (10^{-4} M) and were injected through the electrospray interface at flow rates ranging from 3 to 5 μL/min. In the case of the phenoxide dianion, the reactive nucleophile was masked with a more easily ionized sulfonate group. Under collision-induced dissociation conditions, the precursor readily loses $C_3H_6SO_3$ presumably via an intramolecular cyclization to give the phenoxide dianion (Scheme 4). Typical ESI conditions involved needle potentials from 3.5 to 4.5 kV and heated capillary temperatures from 125 to 200 °C.

Scheme 4. Preparation of Dianion II

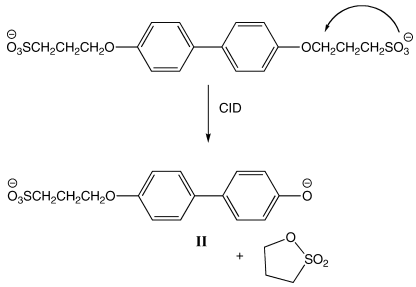

After a short time-delay in which ions were collected, a notched waveform was applied to isolate the ion-of-interest (the dianion) in the ion trap. Once a steady signal was achieved, the neutral reagent was introduced into the helium system via a custom gas-handling system.[13] This is done by injecting a constant flow of reagent (20−400 μL/h) by a syringe pump with the syringe's needle being directed into a measured flow of helium (1000−1500 mL/min). This process allows for rapid vaporization at the needle yielding mixing ratios of 10^2−10^4 (He/reagent). Most of the gas is discarded through a flowmeter, whereas a small amount (~0.1 mL/min) is transferred into the trap. In order to control the helium pressure, the LCQ utilizes a constriction capillary that is designed to maintain 1.75 mtorr of helium in the trap. When combined with the mixing ratio, the ion trap pressure can be used to calculate the reagent's partial pressure (a differential effusion correction is needed).[7] The ion trap pressure is routinely calibrated by collecting data for reactions with established rate constants.[3,9] Once an appropriate flow of the neutral reagent was established, the system was given several minutes for the reagent pressure to equilibrate to a steady state. To analyze the reactions, the LCQ software was set to do a tandem mass spectrometry (MS/MS) scan with no excitation energy and a varying excitation time. Reactions were monitored as a function of time at various flow rates (pressures) of the reagent and branching ratios were determined. Kinetic measurements were performed assuming pseudo first-order conditions because the concentration of the neutral reagent is a constant under these conditions (reagent/dianion =10^5-10^6). Time delays and reagent flows were adjusted to obtain plots that covered two to three half-lives of the reactant ion. Reported rates are measured at three different reagent flow rates and an average of at least ten kinetic runs was collected on two or more days (>30 runs). Kinetic plots showed good linearity and gave correlation coefficients (r^2) greater than 0.98. Product distributions were determined by integrating the areas under the appropriate peaks. In the past, we have shown that the ion trap gives reactivity at near ambient temperature.[4] All alkyl halides were obtained from commercial sources and washed with aqueous $NaHCO_3$ prior to the experiment to remove any acidic impurities.

Computational Methods. Geometries were first modeled using Spartan '10 at the HF/6-31+G(d) level.[28] All other calculations were completed using the GAUSSIAN03 quantum mechanical package.[33] Optimizations were completed at the MP2/6-31+G(d) level. Energies were computed at the MP2/6-31+G(d,p)//MP2/6-31+G(d) level and corrected for the zero-point vibrational energies (ZPE, scaled by 0.9135).[34] In the extended studies of the S_N2 reactions of 1-bromopentane and 3-bromopentane, data are from the MP2/6-31+G(d) level and zero-point energies were not corrected.

ASSOCIATED CONTENT

Supporting Information

Energies and geometries for all relevant species in the computational study are available as well the complete citation for ref 33. This material is available free of charge via the Internet at http://pubs.acs.org.

AUTHOR INFORMATION

Corresponding Author

*E-mail: sgronert@vcu.edu.

Notes

The authors declare no competing financial interest.

ACKNOWLEDGMENTS

Support from the National Science Foundation (CHE-1011771) is acknowledged. K.M.C. thanks the Altria Corp. for a generous fellowship.

REFERENCES

(1) Streitwieser, A. *Solvolytic Displacement*; McGraw-Hill: New York, 1962.
(2) Saunders, W. H., Jr.; Cockerill, A. F., *Mechanisms of Elimination Reactions*; John Wiley & Sons: New York, 1973.
(3) Gronert, S. *Mass Spectrom. Rev.* **2005**, *24*, 100.
(4) Olmstead, W. N.; Brauman, J. I. *J. Am. Chem. Soc.* **1977**, *99*, 4219.
(5) Wladkowski, B. D.; Wilbur, J. L.; Brauman, J. I. *J. Am. Chem. Soc.* **1994**, *116*, 2471.
(6) DePuy, C. H.; Gronert, S.; Mullin, A.; Bierbaum, V. M. *J. Am. Chem. Soc.* **1990**, *112*, 8650.
(7) Gronert, S. *Acc. Chem. Res.* **2003**, *36*, 848.
(8) Gronert, S. *Chem. Rev.* **2001**, *101*, 329.
(9) Gronert, S.; DePuy, C. H.; Bierbaum, V. M. *J. Am. Chem. Soc.* **1991**, *113*, 4009.
(10) Garver, J. M.; Gronert, S.; Bierbaum, V. M. *J. Am. Chem. Soc.* **2011**, *133*, 13894.
(11) Garver, J. M.; Yang, Z. B.; Nichols, C. M.; Worker, B. B.; Gronert, S.; Bierbaum, V. M. *Int. J. Mass Spectrom.* **2012**, *316*, 244.

(12) Gronert, S.; Fagin, A. E.; Wong, L. *J. Am. Chem. Soc.* **2007**, *129*, 5330.
(13) Lum, R. C.; Grabowski, J. J. *J. Am. Chem. Soc.* **1988**, *110*, 8568.
(14) Lum, R. C.; Grabowski, J. J. *J. Am. Chem. Soc.* **1992**, *114*, 9663.
(15) Vayner, G.; Houk, K. N.; Jorgensen, W. L.; Brauman, J. I. *J. Am. Chem. Soc.* **2004**, *126*, 9054.
(16) Ren, J. H.; Brauman, J. I. *J. Am. Chem. Soc.* **2004**, *126*, 2640.
(17) Chen, X.; Regan, C. K.; Craig, S. L.; Krenske, E. H.; Houk, K. N.; Jorgensen, W. L.; Brauman, J. I. *J. Am. Chem. Soc.* **2009**, *131*, 16162.
(18) Flores, A. E.; Gronert, S. *J. Am. Chem. Soc.* **1999**, *121*, 2627.
(19) Gronert, S. *J. Am. Chem. Soc.* **1993**, *115*, 652.
(20) Regan, C. K.; Craig, S. L.; Brauman, J. I. *Science* **2002**, *295*, 2245.
(21) Gronert, S.; Fong, L. M. *Int. J. Mass Spectrom.* **1999**, *192*, 185.
(22) Bartmess, J. E. Negative Ion Energetics Data. In NIST Standard Reference Database Number 69. Mallard, W. G., Linstrom, P. J., Eds.; National Institute of Standards and Technology: Gaithersburg, MD, 2013; http://webbook.nist.gov.
(23) The collision rates of these systems are problematic to characterize by standard approaches. The dianions have two widely spaced charge sites, and the application of ADO theory with a charge of 2 is not a realistic representation of the situation. Using ADO as a general guide, these reactions give predicted collision rates in the range of $3-4 \times 10^{-9}$ cm^3 molecule^{-1} s^{-1}.
(24) Su, T.; Bowers, M. T. In *Gas Phase Ion Chemistry*; Bowers, M. T., Ed.; Academic Press: New York, 1979; Vol. *1*, p 83.
(25) Nettey, S.; Swift, C. A.; Joviliano, R.; Noin, D. O.; Gronert, S. *J. Am. Chem. Soc.* **2012**, *134*, 9303.
(26) Gronert, S.; Fagin, A. E.; Okamoto, K.; Mogali, S.; Pratt, L. M. *J. Am. Chem. Soc.* **2004**, *126*, 12977.
(27) Gronert, S.; Pratt, L. M.; Mogali, S. *J. Am. Chem. Soc.* **2001**, *123*, 3081.
(28) Spartan '10, Wavefunction, Inc.: Irvine, CA.
(29) In this case, the computed free energy of activation favors 1-bromopentane over 3-bromopentane, but by less than that which is seen in the experimental analogue or predicted by considering all pathways.
(30) Manikandan, P.; Zhang, J. X.; Hase, W. L. *J. Phys. Chem. A* **2012**, *116*, 3061.
(31) Wang, H. B.; Zhu, L.; Hase, W. L. *J. Phys. Chem.* **1994**, *98*, 1608.
(32) Chabinyc, M. L.; Craig, S. L.; Regan, C. K.; Brauman, J. I. *Science* **1998**, *279*, 1882.
(33) Frisch, M. J. et al. Gaussian 03, Revision B04; Gaussian, Inc.: Pittsburgh, PA, 2003.
(34) Pople, J. A.; Scott, A. P.; Wong, M. W.; Radom, L. *Isr. J. Chem.* **1993**, *33*, 345.

dx.doi.org/10.1021/jo4013354 | *J. Org. Chem.* 2013, 78, 8606−8613